



## **Active and passive vibration control technology for tri-sonic wind tunnel models**

*YAN Huanhuan<sup>1</sup>, NI Wenbin<sup>1</sup>, WU Junfei<sup>1</sup>, PAN Xiaojun<sup>1</sup>, ZHOU Jian<sup>1</sup>, YAN Wanfang<sup>1</sup>, LIU Sen<sup>1</sup>, WANG Tiejun<sup>1</sup>, ZHANG Jiang<sup>1</sup>*

### **Abstract**

In subsonic and supersonic wind tunnel tests, the commonly used tail brace is a typical concentrated mass cantilever beam structure. In transonic and supersonic flow, the airflow and model support system sometimes undergo severe coupling vibration, and the alternating vibration of the model can have a very adverse impact on the accuracy of the balance measurement system and the reliability and lifespan of the support system. Under a specific high angle of attack, the experiment generates rapid divergent vibrations with obvious resonance characteristics, which cannot achieve the completion of data collection of the angle of attack envelope, and can seriously damage the safety of the test structure and balance system. Passive vibration suppression using non Newtonian materials and tungsten steel support rods, and active vibration suppression using piezoelectric ceramics to achieve the best vibration suppression effect. Due to the advantages of high energy density and rapid response of piezoelectric ceramic materials, the use of piezoelectric ceramic actuators as active vibration suppression technology for wind tunnels has become a research hotspot. Based on the principle of variable stiffness active vibration suppression, an active and passive vibration suppression system was designed in the wind tunnel using stacked piezoelectric ceramic actuators. The main purpose of the system is to solve the serious vibration problems that occur in the model during transonic testing. Based on the analysis of key techniques in model vibration, the design optimization of the layout of the vibration suppressor was achieved. The feasibility of this design method and the performance of the entire vibration suppression system were verified through ground and wind tunnel tests. The test results showed that the vibration suppression system can suppress the impact vibration of the model's supersonic switching vehicle and the vibration caused by aerodynamic structure coupling, and effectively improve the available attack angle of the test, providing a reliable testing technology for the model's supersonic test.

**Keywords** : *large aspect ratio model, vibration control, piezoelectric ceramics, wind tunnel testing, active and passive control*

---

<sup>1</sup> *China Academy of Aerospace Aerodynamics, 17 Yungang West Road, Fengtai District, Beijing, yanhuanhuan15@126.com*



## 1. Introduction

In order to reduce vibration loads, supersonic wind tunnel tests often use release mechanisms, enhanced balance structures and impact resistant devices, advanced wind tunnel multi-stage pressure reducing and other pressure regulating valve control strategies, injection driving to reduce the total starting pressure, using clamp plates to suppress vibration [1], viscoelastic material [2,3,4,5] and adding Tuned Mass Damper [6,7] to passively suppress structural vibration. Each scheme has its own advantages and disadvantages. For production wind tunnels that have already been put into use, the main drawback of the above methods is that they are not universal, and there is a certain lag in the sudden structural vibration phenomenon during wind tunnel testing due to time constraints and equipment transformation difficulties, which cannot effectively solve on-site problems in a timely manner.

Due to the advantages of high energy density and rapid response of piezoelectric ceramic materials, the use of piezoelectric ceramic actuators as active vibration suppression technology for wind tunnels has become a research hotspot. Domestic and foreign research institutions such as NASA [8,9,10], ETW [11,12], Canada NRC [13], Russia TsAGI [14], China Aerodynamics Research and Development Center [15], Avic Aerodynamics Research Institute [16,17], Dalian University of Technology [18,20,20], Nanjing University of Aeronautics and Astronautics [21,22] have gained rich wind tunnel test experience in active vibration suppression of model structures in sub cross flow fields with Ma less than 1. However, there are few literatures about active and passive vibration suppression of models in supersonic flow field flow field with Mach number greater than 1.

In order to solve the serious vibration problem caused by the large slenderness ratio missile models and large lifting surface aircraft model in tri-sonic tests. Passive vibration suppression using non Newtonian materials and tungsten steel support rods, and active vibration suppression using piezoelectric ceramics to achieve the best vibration suppression effect. This scheme uses piezoelectric ceramics based on the piezoelectric effect to achieve variable stiffness active vibration suppression of the balance model support system. Using stacked piezoelectric ceramic actuators, a set of active vibration suppression systems suitable for Ma0.4 to Ma4.0 was designed in the wind tunnel. Combined with the passive vibration suppression of new materials such as D30/PBDMS shear thickening materials and light materials. Based on the analysis of key technology of model vibration, the design optimization of the layout of the vibration suppressor was achieved. The large slenderness ratio missile model was applied in practice in Ma2 and achieved good results.

## 2. Structural vibration analysis

### 2.1. Impact load estimation method

For the estimation of impact load, the time when the impact load occurs is assumed to be the most extreme case, and the calculation is based on the appearance of a normal shock wave on the upper surface of the model head and a normal shock wave at the tail of the model. There are mainly two types of impact theory calculation:

(1) The difference in static pressure between upstream and downstream of the shock wave:

$$P_2 - P_1 = \frac{2\gamma(M^2 - 1)P_0}{(\gamma + 1) \left[ 1 + \frac{\gamma - 1}{2} M^2 \right]^{\frac{\gamma}{\gamma - 1}}}$$

(2) The difference between the static pressure upstream of the shock wave and the total pressure downstream of the shock wave:

$$P_{02} - P_1 = \frac{P_0}{\left(\frac{2\gamma M^2 - \gamma + 1}{\gamma + 1}\right)^{\frac{1}{\gamma-1}} \left(\frac{2 + (\gamma-1)M^2}{(\gamma+1)M^2}\right)^{\frac{\gamma}{\gamma-1}}} - \frac{P_0}{\left(1 + \frac{\gamma-1}{2}M^2\right)^{\frac{\gamma}{\gamma-1}}}$$

In 1962, Maydew [23]:et al. studied the comparison between theoretical and experimental values of classical models and found that the impact load calculated using theoretical formulas magnified the impact load that occurred during the experiment below the Mach number of  $Ma=3$ .the impact load increases from  $Ma=1.0$  and reaches the maximum near  $Ma=3.0$ .

The starting impact load of the model  $F_{Nm}$  in wind tunnel test is a function of Mach number ( $M_a$ ),projected aera of the model ( $S$ )and total pressure ( $P_0$ )when the flow field is established.tri-sonic wind tunnel,  $\gamma=1.4$ ,estimated by static pressure method.

$$F_{Nm} = \frac{7(Ma^2 - 1)P_0}{6[1 + 0.2Ma^2]^{3.5}} S$$

The above methods are only applicable to the estimation of the maximum longitudinal impact load of the model. There has been no more accurate estimation method for axial and lateral impact loads. Adopt the corresponding safety factor method for strength verification in model design.

In practice, model vibration is generated by the coupling of multiple factors. Using accelerometers to measure vibration can obtain real-time and effective data for vibration suppression.

By summarizing the data of vibration caused by blowing in the temporary tri-sonic wind tunnel ,it is found that the large slenderness ratio missile model is prone to vibration in the unsteady state such high angle of attack test, inlet atart-up test, vertical tail buffeting test of finghter at high angle of attack,flutter test of large aspect ratio model, heavy propeller helicopter model test and test mach number of 3,and the maximum pulsation can reach about 20%~30% in severe cases.therefore ,in the design stage, the estimated fluctuating load of 30% of the maximum normal force range of the balance can be used as the basis for structural load design and harmonic response analysis,and at the same time ,the T-38 wind tunnel recorded at Mach 2.5 the transient loads exceed maximum test loads by more than a factor of 2[24]; .appropriate safety factors and nexessary vibration reduction measures should be selected in the overall test design.

## 2.2. selection based on natural frequency of strut to avoid excitation frequency

by using the energy method, the influence of the distributed mass of the elastic elements of the system on the overall vibration characteristics of the system can be compensated,so as to obtain a more accurate natural frequency of the system. In engineering,it is usually assumed that the dynamic deflection curve of a cantilever beam system under free vibration is the same as the static deflection curve generated by static load at its free end.

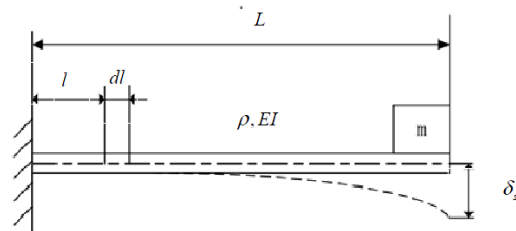


**Fig 1.** dynamic deflection approximation of cantilever beam system[25]

Where  $m'$  is the mass of the cantilever beam. Considering the concentrated mass, the maximum kinetic energy of the whole system is:

$$x_t(t) = x(t) \frac{3Ll^2 - l^3}{2L^3}$$

The undamped natural frequency of the system is

$$\omega_n = \sqrt{\frac{3EI}{L^3 \left( m + \frac{33}{140} m' \right)}}$$

The equivalent mass of the system is defined as

$$M_{eq} = m + \frac{33}{140} m'$$

the condition that other geometric conditions are unchanged, the natural frequency is related to density and Modulus of elasticity .

$$\omega_n = k_1 \sqrt{\frac{E}{m}} = k_2 \sqrt{\frac{E}{\rho}}$$

According to the theoretical formula, the corresponding material characteristics are sorted out and summarized. Under the condition that the foot strength requirements are consistent with the geometric dimensions, the F-141 material is Material as a benchmark for comparative analysis, assuming that the natural frequency of other materials to avoid 90%~110% of the frequency of F141 is regarded as avoiding the resonance interval. It can be seen from the comparison table that the lateral forces of carbon fiber, iron-titanium alloy and tungsten steel material, glass fiber reinforced plastic, and D30 shear thickening material can all be used.

Avic Aerodynamics Research Institute carries out vibration reduction design of carbon fiber materials [26].Serbia Institute of Military Technology VTI used 90WC-10Coalloy tungsten steel and Armco Ph 13.8 Mo steel composite strut in T-38 wind tunnel for vibration reduction design[27]. This proves the feasibility of theoretical analysis of material vibration reduction in this paper.

**Table 1.** Performance comparison chart of main materials

serial Number	material	bending strength /MPa	density	Elastic modulus /E	$\omega = \sqrt{\frac{E}{\rho}}$	$\omega_i/\omega_{F141}$
			kg/m <sup>3</sup>	GPa		
1	F141(18Ni(250))	1862	8000	187.25	4838	1.00
2	18Ni(300)	1930	8000	190	4873	1.01
3	18Ni(350)	2275	8000	200	5000	1.03
4	30CrMnSiA	1080	8000	196	4950	1.02
5	35CrMnSiA	1620	8000	206	5074	1.05
6	0Cr17Ni4Cu4Nb(17-4PH)	1313	8000	207	5087	1.05
7	GH141high-temperaturealloy	1070	8270	207	5003	1.03
8	Nikro 128ferro-titanium	1200	6600	294	6674	1.38
9	Nikro 143ferro-titanium	1450	6700	280	6465	1.34
10	tungsten steel YL50	3000	14300	420	5419	1.12
11	tungsten steel YL80	3800	14100	410	5392	1.11
12	tungsten steel YL90.6	5300	13000	330	5038	1.04
13	lead(Pb1)	2.5	11340	17	1224	0.25
14	carbon fibre T300	3530	1760	230	11432	2.36
15	carbon fibreT700	4900	1800	230	11304	2.34
16	carbon fibreT800	5880	1800	294	12780	2.64
17	Aluminum alloy 7075	540	2820	71.7	5042	1.04
18	glass fiber reinforced plastics(polyamideimide)	255	1610	8.6	2311	0.48
19	Piezoelectric actuator		7.5	19	50332	10.40



**Fig 2.** schematic diagram of carbon fiber material model

According to the reasonable design, for the same set of small aspect ratio aircraft models in tri-sonic wind tunnel, the amplitude angle range is reduced from about 5 to 1 under the same wind tunnel blowing condition by replacing the steel model of 30CrMnSiA with the model made of 7075 aluminum alloy. the natural frequency increases by about 45%.

**Table 2.** Comparison of natural frequencies of different materials in small aspect ratio aircraft model

Frequency mode	1	2	3	4	5	6
Aluminum alloy 7075(Hz)	24.2	24.9	71.4	78.7	102.2	175.4
30CrMnSiA(Hz)	16.6	16.9	48.3	54.0	82.2	174.1

**2.3. shock resistance and vibration reduction of non-Newtonian fluid materials based on shear thickening effect**

When  $Ma=0.6\sim 1.15$ , the normal force pulsation of the large slenderness ratio missile model is obviously enhanced in the angle of attack of 60 degrees to 120 degrees, while the lateral force pulsation is obviously increased in the range of 45 degrees to 75 degrees and 105 degrees to 150 degrees. The large lateral force and normal force pulsation are easy to cause the model vibration. At high angle of attack, the lateral force is  $1/4\sim 1/2$  of the normal force, and the lateral aerodynamic force has obvious dominant frequency (400-1000Hz) in the range of attack angle of 45-165[28].

Therefore, from the point of view of vibration suppression strategy, the high-angle-of-attack missile model needs low frequency in pitch direction (below 100Hz) and high frequency in yaw direction (400-1000Hz) to simultaneously suppress vibration.

Domestic boric acid modified hydroxyl-terminated polysiloxane (PBDMS) is a kind of clay-like silicon polymer with shear thickening effect. On the premise of maintaining good flexibility, excellent shock absorption, impact resistance, explosion protection and other properties are obtained

Because piezoelectric ceramics are mainly used to suppress the vibration below 30Hz, D3O/PBDMS non-Newtonian fluid shear thickening gel is used to design the vibration reduction for the lateral force of the missile at high angle of attack and the vibration of the abdominal support above 30Hz.



**Fig 3.** Domestic boric acid modified hydroxyl-terminated polysiloxane (PBDMS)

Three different materials are selected to analyze the application effect of model vibration reduction. Firstly, the dynamic compressive properties of three kinds of shear thickening materials at different strain rates were tested by Hopkinson pressure bar technology. According to the test data, the

dynamic impact mechanical response of materials and the variation law of material properties with strain rates were analyzed. Through the stress-strain curves of materials, all three materials have obvious strain rate sensitivity. Through the test, its response time is about 1/900 second to 1/2300 second, and the stress is in 1.3MPa to 9.67MPa. The strain is between 28% and 35%.

The ground test was carried out on a large slenderness ratio missile model. In the missile head cavity, the ground hammer test was carried out with shear thickening gels filled with different materials. Test results show that the orange PBDMS shear thickening material can reduce the vibration by about 81.7%. It has a certain effect on restraining the starting & stopping transient load of the temporary trisonic wind tunnel. However, it can't significantly reduce the damping and attenuation time, which may be caused by the temperature or the volume deformation caused by the over-filling of PBDMS shear thickening gel in the missile head. Further verification tests were carried out on the PBDMS shear thickening gel filled in the model cavity.

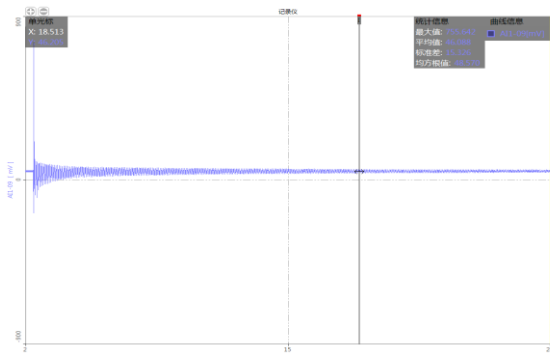


**Fig 4.** Excitation response curve of non-shear thickening material in missile head cavity

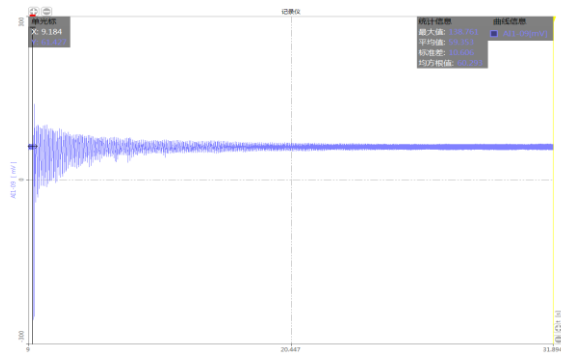


**Fig 5.** Excitation response curve of orange shear thickening material in missile head cavity

**Table 3.** PBDMS shear thickening test in missile head cavity vibration reduction result

	transparent PBDMS	red PBDMS	orange PBDMS	non-shear material	tickening
The maximum value	292.3	487.32	138.76	755.64	
Standard deviation	9.05	8.34	10.60	15.32	
Root mean square	61.46	60.9	60.29	48.57	

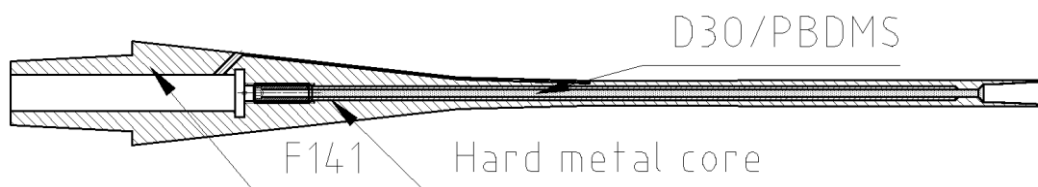


**Fig 6.** Schematic diagram of the strut structure of F141 combined with tungsten steel alloy and filled with PBDMS shear thickening material

According to the above theoretical analysis and ground test, we designed an active and passive vibration suppression system for the missile model with large slenderness ratio. The passive vibration suppression scheme adopted a combination of cemented carbide tungsten steel strut and F141(18Ni(250)) strut, and a certain proportion of D30/PBDMS material was filled in the inner cavity of the warhead and the strut for passive vibration suppression.

Although passive vibration suppression can achieve certain results, the benchmark is suitable for working conditions. The scope is small and the efficiency is low. In order to achieve efficient vibration suppression, a method based on the active vibration suppression system of piezoelectric ceramics is designed.

### 3. Design of Active and Passive Vibration Suppression System

#### 3.1. Basic principles of piezoelectric ceramic vibration suppression

Active vibration suppression can achieve real-time vibration suppression through real-time feedback of vibration. By providing excitation signals with the same amplitude, opposite phase, and same frequency as the original vibration, and overlaying them with the original vibration, amplitude reduction is achieved, achieving the goal of actively suppressing vibration; Due to the small size, high output, and rapid response of piezoelectric ceramics, active vibration reduction methods based on piezoelectric ceramics have become the mainstream direction of wind tunnel tail support vibration suppression research.

Active vibration suppression methods include vibration suppression at the head of the support rod and vibration suppression at the root of the support rod. Due to the difficulty in arranging piezoelectric ceramics at the head of wind tunnels with a length of 1.2 meters or less, piezoelectric ceramics are often placed at the tail for active vibration suppression. For large wind tunnels with a length of more than 2 meters, a combination of head and tail vibration suppression can be used; Active vibration suppression system such as ETW.

#### 3.2. Design of Active Vibration Suppression Structure for Piezoelectric Ceramics

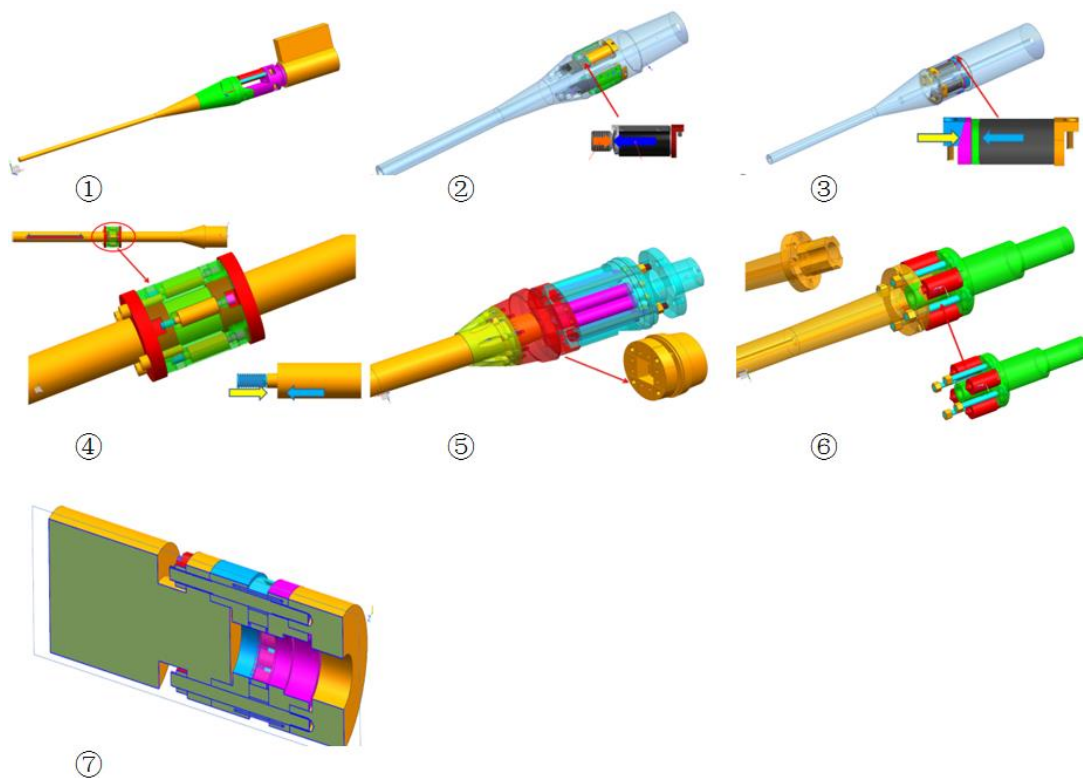


**Fig 7.** Scheme of Active Vibration Suppression System Based on Piezoelectric

According to domestic and foreign literature on the principle of active vibration suppression and piezoelectric ceramic actuators, the following seven overall structural design schemes are mainly designed. Each of the above structures has its advantages and disadvantages, in order to achieve a set of active vibration suppression systems and meet the requirements of different support rods. Taking into account the advantages and disadvantages of the above structures, a detailed optimization design is carried out based on the concept of "fine adjustment of pre tightening force on inclined surfaces+embedding of piezoelectric ceramics+replaceable support rods".

### 3.3. Structural optimization design of active vibration suppression system

Based on wind tunnel test data, simplify the wind tunnel model into a 40kg disk structure for static load analysis of the support rod system. Under maximum load conditions, the maximum stress value of the model is about 635Mpa, and F141 (18Ni-250) material is selected for processing; The yield strength of the material is 1800 MPa, with a safety factor of 2.8. The support rod meets the static strength requirements under extreme loads.

Load analysis was conducted on different output structures such as piezoelectric ceramic ball heads, square heads, and threaded heads. In order to increase the contact area and reduce stress loads, a large circular arc surface structure was designed for use.

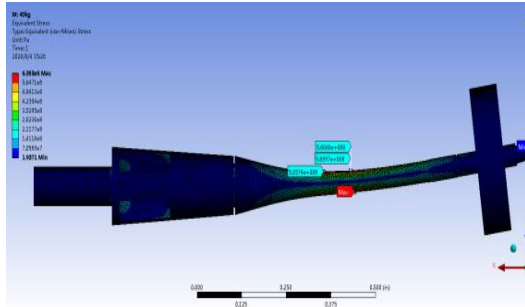


Fig 8. static analysis of the support rod

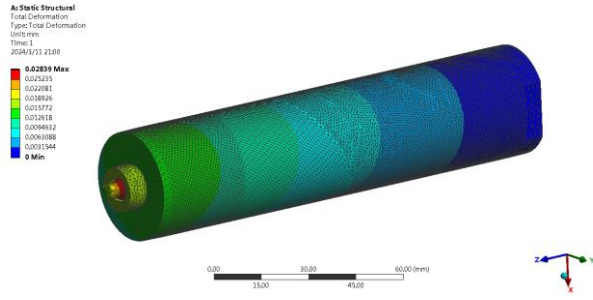


Fig 9. static analysis of the piezoelectric ceramic

### 3.4. Modal Analysis of Aircraft Model for Active Vibration Suppression System

Perform modal analysis on the entire "model balance support rod" system. Through modal analysis, it was found that the first and second modal frequencies are very similar, the vibration modes are orthogonal, and the third, fourth, and fifth orders are similar. In the wind tunnel flow field environment, the model system is coupled with wind load excitation, mainly producing severe resonance in the pitch direction. The compound resonance phenomenon of the model is easily caused near the two frequencies.

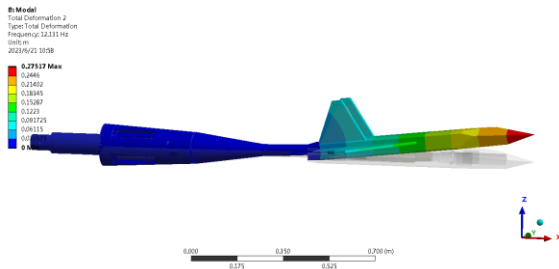


Fig 10. F-22-like aircraft Modal Analysis(12.13Hz)

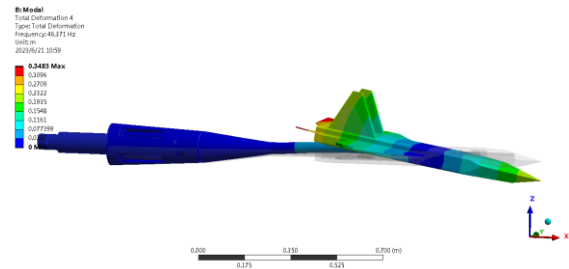


Fig 11. F-22-like aircraft Modal Analysis(46.37Hz)

Table 4. Modal Analysis of the F-22-like model

Modal	frequency Hz	state
1	11.96	System left and right vibrations
2	12.13	System pitch up and down vibration
3	44.21	Aircraft Left and Right Vibration
4	46.37	Aircraft pitch vibration
5	49.91	Aircraft Rolling Vibration
6	126.53	Horizontal tail reverse vibration

According to the results of wind tunnel experiments, as pitch vibration is the main formation, an active vibration suppression system is designed to meet the technical requirements of its vibration mode, frequency, load, displacement, etc.



### 3.5. Analysis of Harmonic Response of Aircraft Model for Active Vibration System

Based on the experimental pulsating load, a sinusoidal load of 3000N is designed for harmonic response load analysis. A sinusoidal excitation of  $F_t = F_{\max} \cdot \sin(2\pi f \cdot t)$  is applied at the center of mass of the model for frequency sweep. As shown in the figure, when  $f$  is greater than 11.4Hz near the first frequency, the structural vibration acceleration increases significantly, and the support rod exceeds the strength limit, which is highly likely to cause structural damage.

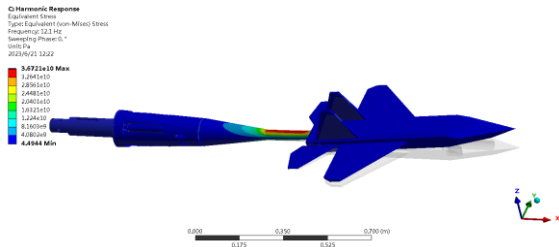


**Fig 12.** 11.4Hz Sweep Frequency Structure Strength

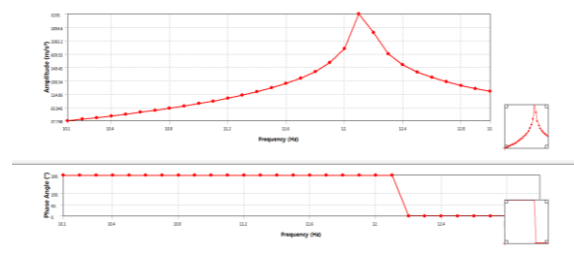


**Fig 13.** Frequency response analysis acceleration response diagram

### 3.6. acceleration sensor design

According to the harmonic response analysis of different models and the vibration data analysis of previous models, the miniature single-component acceleration sensor is selected to be built near the center of the model to detect and feedback the vibration in pitch and yaw directions. The design and application are mainly carried out in two ways: split octahedral acceleration sensor platform and integration of acceleration sensor and balance.

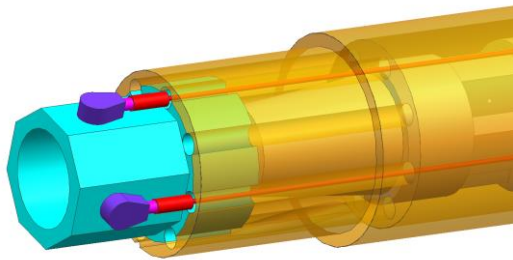


**Fig 14.** octahedral acceleration sensor platform

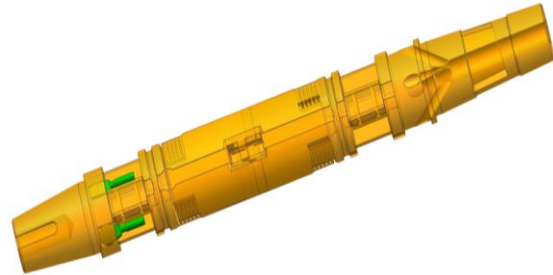


**Fig 15.** schematic diagram of integrated design acceleration and balance



**Fig 16.** physical diagram of integrated design acceleration sensor and balance

### 3.7. Ground Test of Active Vibration for Large Slenderness Ratio missile Models

According to previous wind tunnel test results, large slenderness ratio elastic models are prone to structural resonance due to their large slenderness ratio and small diameter of support rods. According to the experiment, wind tunnel tests were conducted on the ground model of large slenderness ratio projectiles. The slenderness ratio of the model is about 20;

The vibration mode is excited by hammering method, and the free vibration attenuation time of the model is about 30s when the active vibration damper is not turned on. The vibration suppressor time under light load and heavy load conditions is 0.8s and 1.82s respectively; After the vibration suppressor is turned on, the attenuation time is reduced by 85% to 92%.

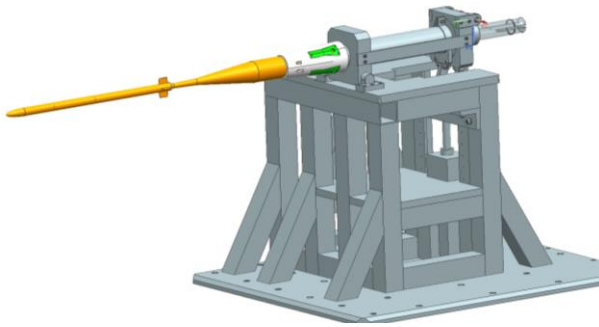


**Fig 17.**Active Vibration Test Device for Large Slenderness Ratio Models

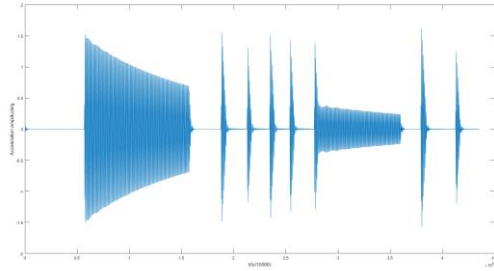


**Fig 18.**Active vibration suppression results

### 3.8. Active Vibration Suppression Ground Test of High Lift Surface Aircraft Models

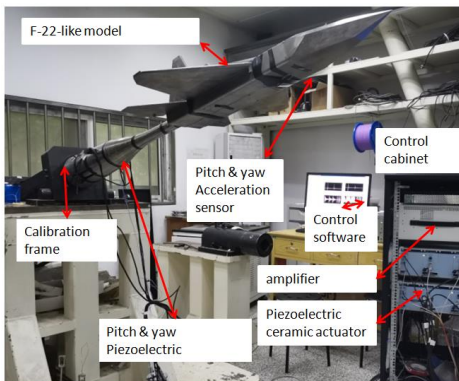


**Fig 19.**Physical diagram of active vibration system for F22-like aircraft model

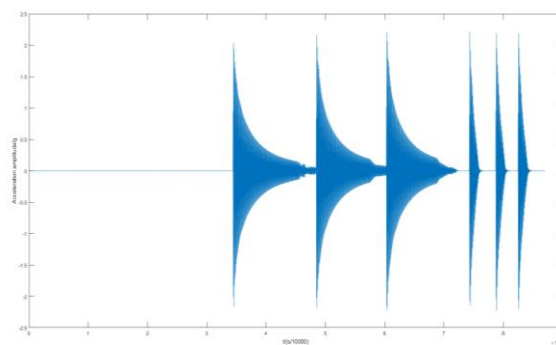


**Fig 20.**Active vibration suppression ground effect diagram

According to previous wind tunnel test results, aircraft models with high lift surfaces are prone to structural resonance in tri-sonic fields due to their large model mass and relatively small support rod diameter. Complete the ground F-22 like aircraft model test according to the experiment.

By simulating the combined attitude of  $0^\circ -15^\circ$  attack angle and  $0^\circ -360^\circ$  roll angle, on the calibration frame, the vibration suppression time of the active vibration suppression system based on piezoelectric ceramics is less than 2 s.

## 4. Conclusion

A set of active vibration suppression system was designed in the tri-sonic wind tunnel, with the main purpose of solving the serious vibration problems that occur in transonic tests with large slenderness ratios. Based on the analysis of key techniques in model vibration, the design optimization of the layout of the vibration suppressor was achieved. Through wind tunnel tests, the feasibility of this design method and the performance of the entire vibration suppression system were verified. The test results showed that at  $Ma=2.5$ , for the pitch direction vibration of the large slenderness ratio model, the vibration suppression system can suppress the supersonic switching vibration of the model and the vibration caused by aerodynamic structure coupling, and effectively improve the available angle of attack for the test. This provides a reliable experimental technology for the supersonic test of the large slenderness ratio model.

## References

1. Liu Qi, LIU Changqing, LI Zengjun. Design of impingement attenuation device for supersonic wind tunnel test models [J]. Journal of Aerospace Power, 2023, 38(2): 364-370.

2. Koryakin A. N. Application of a dynamic vibration damper in aircraft models tested in a wind tunnel // Journal of "Almaz – Antey" Air and Space Defence Corporation. 2020. No. 4. P. 62–68. <https://doi.org/10.38013/2542-0542-2020-4-62-68>
3. Jiahao PAN, Zhanqiang LIU, Xiping KOU, Qinghua SONG. Constrained layer damping treatment of a model support sting[J] Chinese Journal of Aeronautics. (2021), 34(8): 58–64
4. M Roger. Reduction of Dynamic Response of a Wind Tunnel Sting Mount Using a Hub Damper Unit [J]. AIAA 2010-1307
5. Sean Hsu. Reduction of Dynamic Response of a Wind Tunnel Sting Mount Using Co-cured Composite and iscoelastic Materials [J]. AIAA 2010-1308.
6. IGOE W B. Reduction of wind-tunnel-model vibration by means of a tuned damped vibration absorber installed in the model: NASA TMX-1606 [R]. Hampton: NASA, 1968.
7. GAO Dapeng. Research on Vibration Damping of Large Low Speed Wind Tunnel Test Model Based on TMD [D] Mianyang: Southwest University of Science and Technology, 2018.12
8. WB Igoe, FT Capone. Reduction of Wind Tunnel Model Vibration by Means of a Tuned Damped Vibration Absorber Installed in a Model [J]. NASA TMX-1606, July 1968.
9. S Balakrishna. Development of a Wind Tunnel Active Vibration Reduction System [J]. AIAA, 2007-961.
10. BALAKRIS HNA S, BUTLER D, ACHESON M, et al. Design and performance of an active sting damper for the NASA common research model[C] 49th AIAA Aerospace Sciences Meeting. American Institute of Aeronautics and Astronautics, Reston, VA . 2011.
11. H Fehren, U Gnauert, R Wimmel. Validation testing with the active damping system in the European Transonic Wind tunnel. AIAA 2001-00610.
12. EUROPEAN TRANSONIC WIND TUNNEL (ETW) NEWS. NO.12, DECEMBER, 2004.
13. Pereira, J. Development of an active damping system for use with a single strut mount [C] // Proceedings of the 54th AIAA Aerospace Sciences Meeting. San Diego: AIAA, 2016.
14. Strenkov. Typical technical requirements to Tuned Mass Damper of a model during the test on the system in WT [J]. AIAA 2010-1452.
15. YU Li, YANG Xinghua, KOU Xiping, et al. Experiment on Active Vibration Reduction System for Transonic Wind Tunnel Model[J]. Journal of Nanjing University of Aeronautics & Astronautics, 2019, 51 (4) : 526-533.
16. LIU Xinchao, LIU Yu, XU Lingsong. Application and research of active vibration suppression technology based on piezoelectric ceramics in wind tunnel tests[C], in Chinese. Chinese Mechanics Conference, HangZhou 2019
17. CUI Xiaochun, Aerodynamic performance and test capability of 2.4m continuous transonic wind tunnel[R] MianYang, Sichuan, 2022.1.21
18. LIU Wei, BI Xiao-dan, JIA Zhen-yuan, LIU Wei-guo. Design and experiment on active damper of wind tunnel model[J]. Optics and Precision Engineering. Vol.23.No.10.Oct.2015
19. Mengde Zhou. Active Vibration Suppression of the Cantilever Sting for Wind Tunnel Models with Piezoelectric Control[C]. Proceedings of the 2019 IEEE/ASME International Conference on Advanced Intelligent Mechatronics Hong Kong, China, July 8-12, 2019
20. Wei LIU, Mengde ZHOU Zhengquan WEN. An active damping vibration control system for wind tunnel models[J]. Chinese Journal of Aeronautics, (2019), 32(9): 2109–2120
21. CHEN Wei-dong, SHAO Min-qiang, YANG Xing-hua. experimental evaluation of an active vibration control system for wind tunnel aerodynamic models[J] Journal of Vibration Engineering. Vol20.No.1, Feb.2007
22. Xing Shen , Yuke Dai, Mingxuan Chen. et. al Active Vibration Control of the Sting Used in Wind Tunnel[J] Comparison of Three Control Algorithms. Shock and Vibration Volume 2018

23. Hidetoshi HJIMA, Effect of several parameters on starting/stopping loads in a supersonic wind tunnel.JAXA Research and development Report. JAXA –RR-05-048.2006
24. Djordje Vuković.LIVING WITH SUPERSONIC STARTING LOADS IN THE T-38 TRISONIC WIND TUNNEL OF VTI[C] 29<sup>th</sup> Congress of the International Council of the Aeronautical Sciences.St.Petersburg,Russia,September 7-12,2014
25. LIU Weixiao.Research on the Energy-fuzzy Based Active Vibration Control of a Cantilever-like Structure Excited by Aerodynamic Loads[D] Dalian University of Technology.2018.5
26. Si-Peng Li,Yue Xu. Investigation of Vibration Characteristics of Wind Tunnel Rigid Model Based on Material Optimization[C] APISAT2023. Lingshui ,Hainan, China.2023.10.16-17
27. Dušan Čurčić ,Marija Samardžić. Model sting support with hard metal core for measurement in the blowdown pressurized wind tunnel[J]. Measurement 79 (2016) 130–13
28. Wang Fangjian,Wang Hongwei,et.al subsonic unsteady aerodynamic characteristics on slender revolutionary body at extra-wide angle-of-attack [C] the 2nd chinese conference of aerodynamics.Tianjin,china,2023.3